QCD Analysis of the Polarized DIS World Data

Johannes Blümlein and Helmut Böttcher

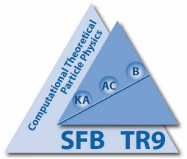

- Data
- The NLO Analysis and Fit Results
- Polarized PDFs
- Λ_{QCD} and $\alpha_s(M_Z^2)$
- Higher Twist Contributions
- Conclusions

DESY 09-131

The Data

Experiment	x–range	Q^2–range $[GeV^2]$	data points type	data points #	$\mathcal{N}_i$
E143(p)	0.027 – 0.749	1.17 – 9.52	g_1/F_1	82	0.963
HERMES(p)	0.026 – 0.731	1.12 – 14.29	A_1	37	0.970
E155(p)	0.015 – 0.750	1.22 – 34.72	g_1/F_1	24	1.003
SMC(p)	0.004 – 0.484	1.14 – 72.10	A_1	59	0.960
EMC(p)	0.015 – 0.466	3.50 – 29.5	A_1	10	0.964
CLAS1(p)	0.125 – 0.575	1.10 – 4.16	A_1	10	1.010
CLAS2(p)	0.292 – 0.592	1.01 – 4.96	g_1/F_1	191	1.030
COMPASS(p)	0.005 – 0.568	1.10 – 62.10	A_1	15	0.955
proton				428	
E143(d)	0.027 – 0.749	1.17 – 9.52	g_1/F_1	82	0.960
HERMES(d)	0.026 – 0.731	1.12 – 14.29	A_1	37	0.970
E155(d)	0.015 – 0.750	1.22 – 34.79	g_1/F_1	24	0.979
SMC(d)	0.004 – 0.483	1.14 – 71.76	A_1	65	0.998
COMPASS(d)	0.005 – 0.566	1.10 – 55.30	A_1	15	0.952
CLAS1(d)	0.125 – 0.575	1.01 – 4.16	A_1	10	1.003
CLAS2(d)	0.298 – 0.636	1.01 – 4.16	g_1/F_1	662	1.014
deuteron				895	
E142(n)	0.035 – 0.466	1.10 – 5.50	A_1	33	0.989
HERMES(n)	0.033 – 0.464	1.22 – 5.25	g_1	9	0.970
E154(n)	0.017 – 0.564	1.20 – 15.00	g_1	17	0.980
JLAB(n)	0.330 – 0.600	2.71 – 4.83	g_1	3	1.000
neutron				62	
total				1385	

Table 1: Number of data points on A_1, g_1/F_1 or g_1 for $Q^2 > 1.0\ GeV^2$ and $W^2 > 3.24\ GeV^2$ used in the present QCD analysis. For each experiment are given the x and Q^2 ranges, the type of quantity measured, the number of data points for each given target, and the fitted normalization shifts $\mathcal{N}_i$ (see text).

Evolution Equations

$$\left[M\frac{\partial}{\partial M} + \beta(g)\frac{\partial}{\partial g} - 2\gamma_\psi(g)\right] F_i(N) = 0$$

$$\left[M\frac{\partial}{\partial M} + \beta(g)\frac{\partial}{\partial g} + \gamma_\kappa^N(g) - 2\gamma_\psi(g)\right] f_k(N) = 0$$

$$\left[M\frac{\partial}{\partial M} + \beta(g)\frac{\partial}{\partial g} - \gamma_\kappa^N(g)\right] C_j^k(N) = 0$$

CALLAN–SYMNANZIK equations for mass factorization
$\equiv$ ALTARELLI–PARISI evolution equations

x-space :

$$\frac{d}{d\log(\mu^2)} \begin{pmatrix} q^+(x,Q^2) \\ G(x,Q^2) \end{pmatrix} = \frac{\alpha_s}{2\pi} \boldsymbol{P}(x,\alpha_s) \otimes \begin{pmatrix} q^+(x,Q^2) \\ G(x,Q^2) \end{pmatrix}$$

$$\boldsymbol{P}(x,\alpha_s) = \boldsymbol{P}^{(0)}(x) + \frac{\alpha_s}{2\pi}\boldsymbol{P}^{(1)}(x) + \left(\frac{\alpha_s}{2\pi}\right)^2 \boldsymbol{P}^{(2)}(x) + \ldots$$

The NLO Fit Results

Δu_v	η	0.928 (fixed)	$\Delta\bar{q}_s$	η	-0.417 $\pm$ 0.079
	a	0.239 $\pm$ 0.027		a	0.365 $\pm$ 0.164
	b	3.031 $\pm$ 0.178		b	8.080 (fixed)
	ρ	0.0 (fixed)		ρ	0.0 (fixed)
	γ	27.64 (fixed)		γ	0.0 (fixed)
Δd_v	η	-0.342 (fixed)	ΔG	η	0.461 $\pm$ 0.430
	a	0.128 $\pm$ 0.068		a	$a_{\Delta\bar{q}_s} + 1$
	b	4.055 $\pm$ 0.879		b	5.610 (fixed)
	ρ	0.0 (fixed)		ρ	0.0 (fixed)
	γ	44.26 (fixed)		γ	0.0 (fixed)
$\Lambda^{(4)}_{QCD} = 243 \pm 62$ MeV			$\chi^2/NDF = 1537/1377 = 1.12$		

Table 2: Final parameter values and their statistical errors at the input scale $Q_0^2 = 4.0\ GeV^2$.

The Correlation Matrix

	$\Lambda^{(4)}_{QCD}$	a_{u_v}	b_{u_v}	a_{d_v}	b_{d_v}	η_{sea}	a_{sea}	η_G
$\Lambda^{(4)}_{QCD}$	**3.85E-3**							
a_{u_v}	-4.08E-4	**7.55E-4**						
b_{u_v}	-1.14E-3	4.30E-3	**3.18E-2**					
a_{d_v}	2.75E-3	-9.39E-4	-4.44E-3	**4.61E-3**				
b_{d_v}	2.38E-2	-8.34E-3	-1.03E-2	4.51E-2	**7.73E-1**			
η_{sea}	1.79E-3	-7.20E-4	-3.79E-3	2.38E-3	2.23E-2	**6.32E-3**		
a_{sea}	-5.65E-3	3.04E-3	1.65E-2	-8.26E-3	-7.39E-2	8.07E-4	**2.70E-2**	
η_G	-1.96E-2	8.32E-3	4.25E-2	-2.16E-2	-1.68E-1	-2.21E-2	4.17E-2	**1.85E-1**

Table 3: The covariance matrix for the $7+1$ parameter NLO fit based on the world asymmetry data.

The Polarized PDFs @ $Q^2 = 4$ GeV^2

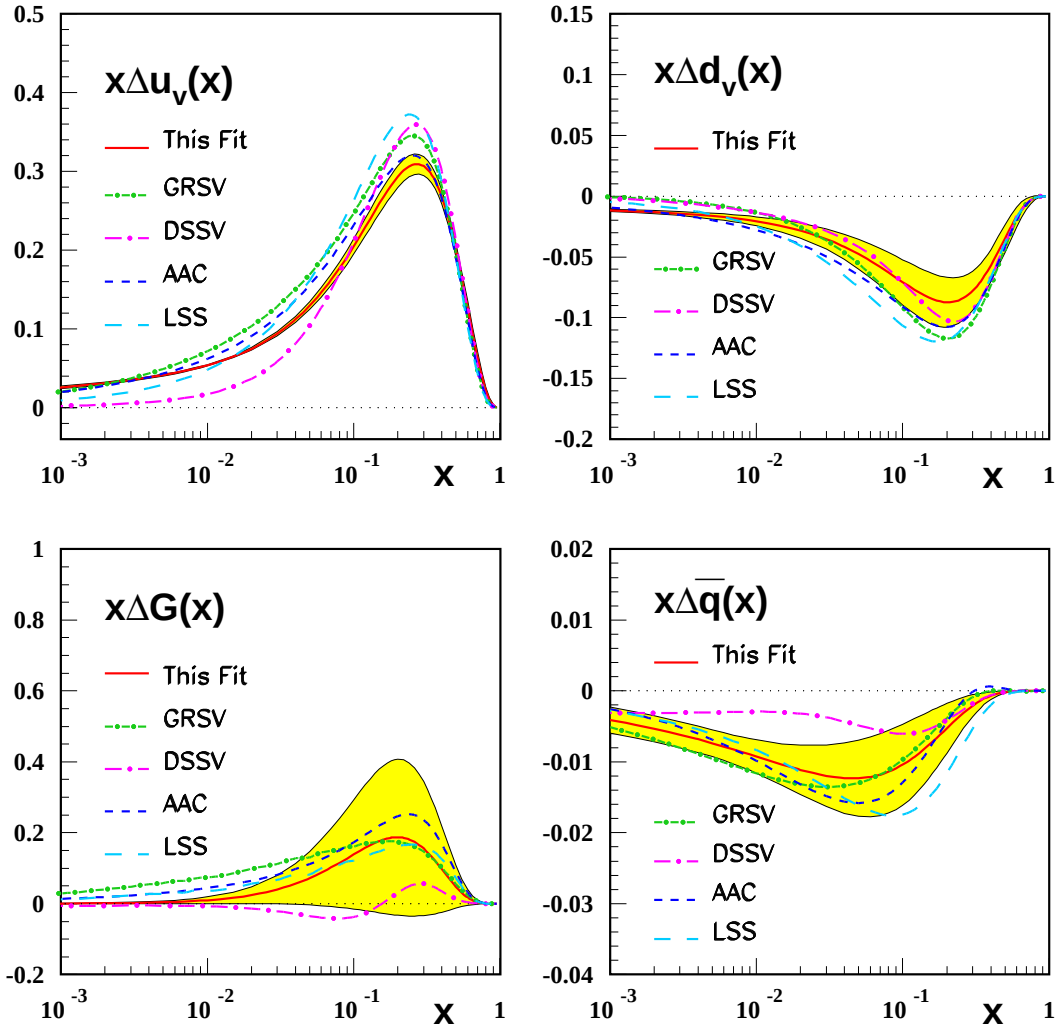

Figure 1: NLO polarized parton distributions at the input scale $Q_0^2 = 4.0$ GeV^2 (solid line) compared to results obtained by GRSV (dashed–dotted line) , DSSV (long dashed–dotted line) , AAC (dashed line) , and LSS (long dashed line) . The shaded areas represent the fully correlated 1σ error bands calculated by Gaussian error propagation.

The Gluon Distribution

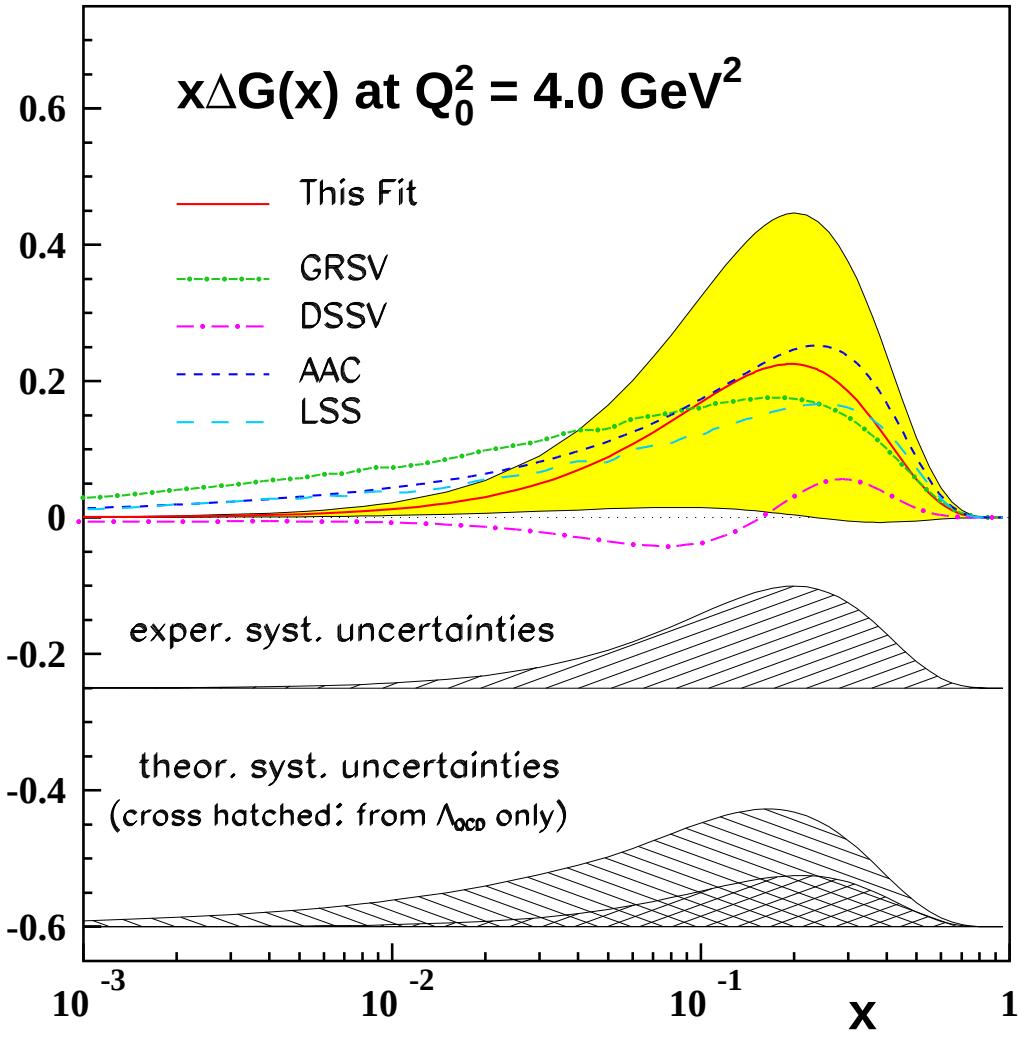

Figure 2: The polarized parton density $x\Delta G(x)$ at $Q_0^2 = 4.0$ GeV^2 as function of x (solid line). The shaded area is the fully correlated 1σ statistical error band and the hatched areas are the systematic uncertainties. Results from GRSV (dashed–dotted line), DSSV (long dashed–dotted line), AAC (dashed line), and LSS (long dashed line) are shown for comparison.

The Singlet Distribution

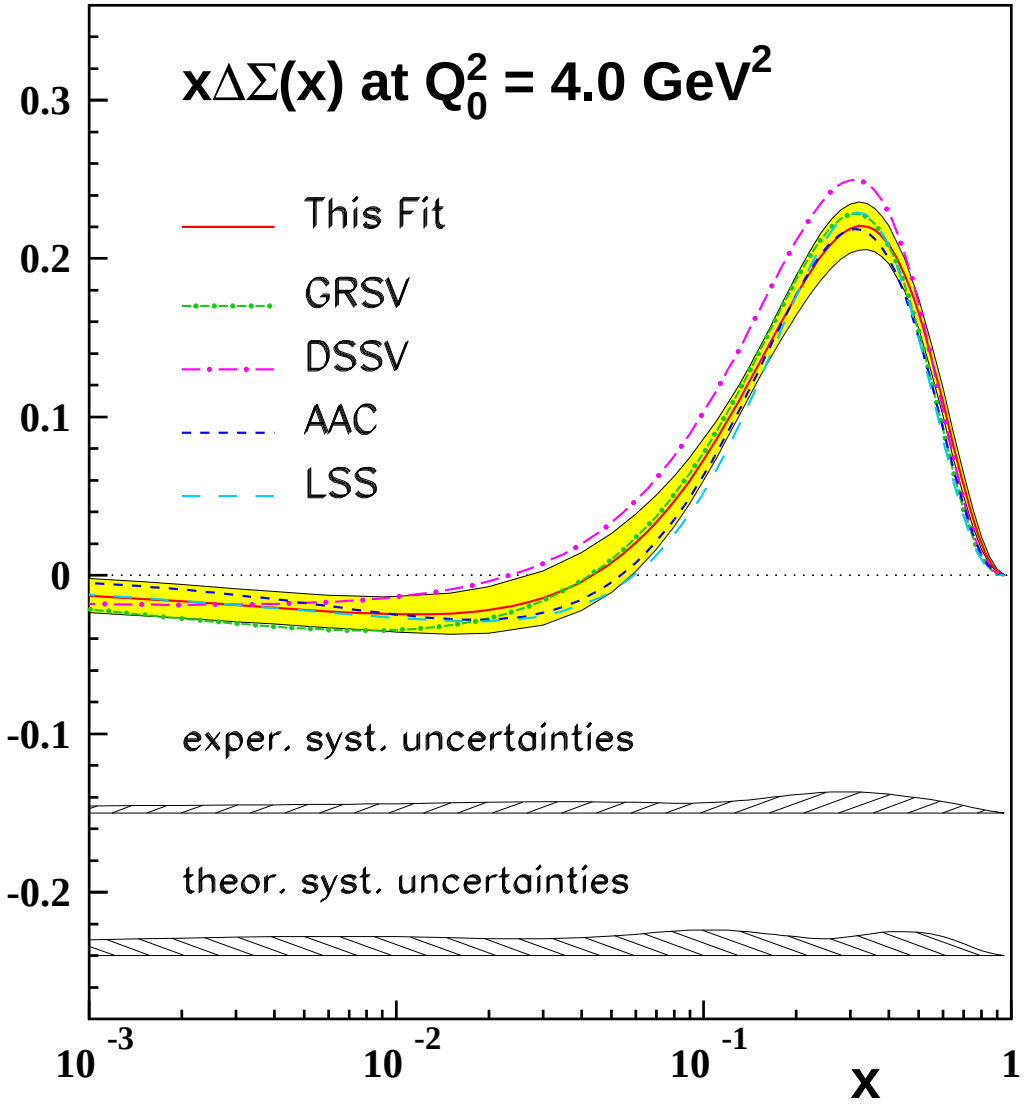

Figure 3: The polarized parton density $x\Delta\Sigma(x)$ at $Q_0^2 = 4.0$ GeV^2 as function of x (solid line). The shaded area is the fully correlated 1σ statistical error band and the hatched areas are the systematic uncertainties. Results from GRSV (dashed–dotted line), DSSV (long dashed–dotted line), AAC (dashed line), and LSS (long dashed line) are shown for comparison.

The Fit and the Data

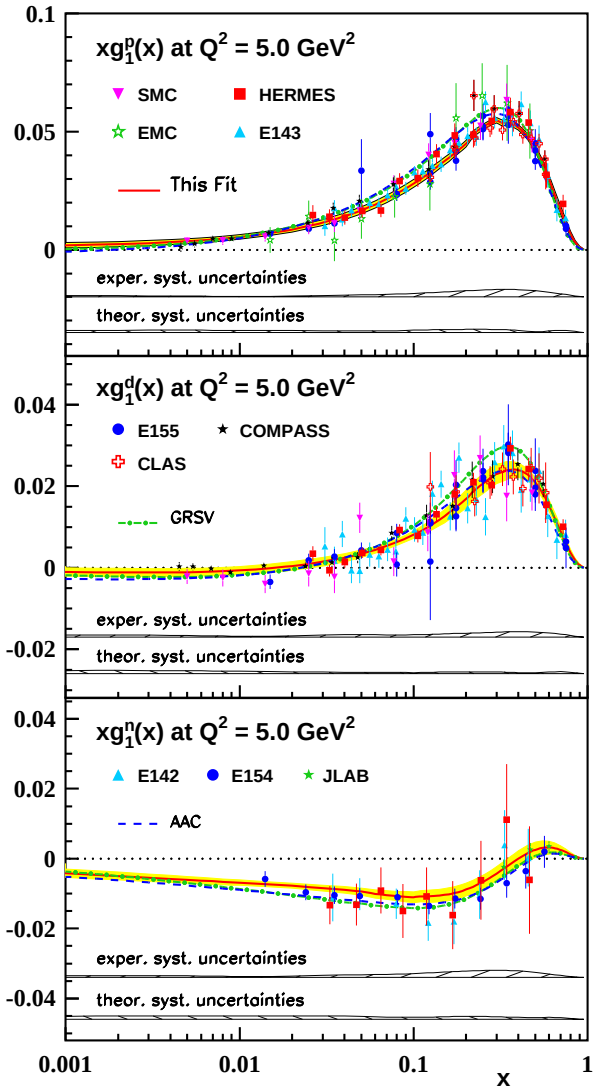

Figure 4: The spin–dependent structure functions $xg_1^p(x)$, $xg_1^d(x)$ and $xg_1^n(x)$ as function of x. The experimental data are evolved to a common value of $Q^2 = 5$ GeV^2. The error bars shown are the statistical and systematic ones added in quadrature. The experimental distributions are well described (solid curve) within the statistical (shaded areas) and systematic (hatched areas) error bands. Shown for comparison are the curves obtained by GRSV (dashed-dotted) and AAC (dashed).

The Fit and the Data

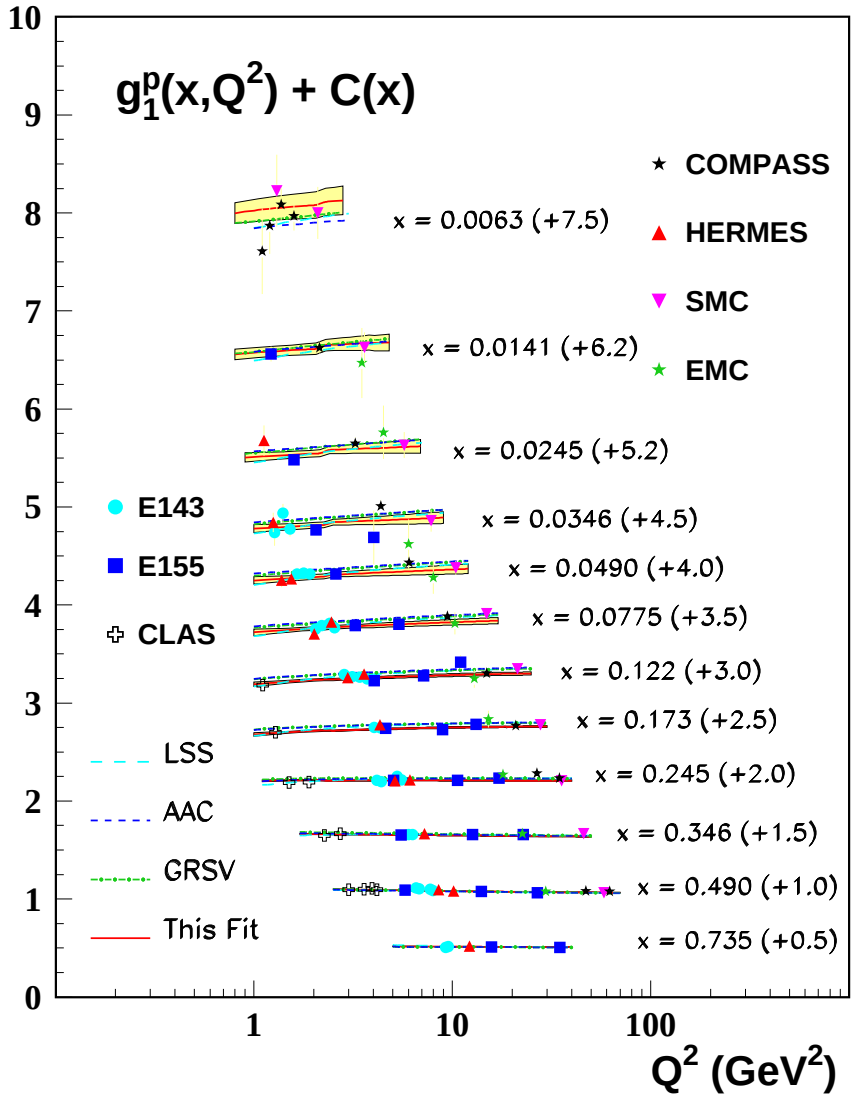

Figure 5: The spin–dependent structure functions $xg_1^p(x)$, $xg_1^d(x)$ and $xg_1^n(x)$ as function of x. The experimental data are evolved to a common value of $Q^2 = 5$ GeV^2. The error bars shown are the statistical and systematic ones added in quadrature. The experimental distributions are well described (solid curve) within the statistical (shaded areas) and systematic (hatched areas) error bands. Shown for comparison are the curves obtained by GRSV (dashed-dotted) and AAC (dashed).

$\alpha_s(M_Z^2)$

S. Alekhin, J.B., S. Klein, S. Moch, Phys.Rev.**D81** (2010) 014032

$$\frac{\delta\alpha_s(M_Z^2)}{\alpha_s(M_Z^2)} \approx 1.2\%$$

	$\alpha_s(M_Z^2)$	
ABKM	0.1135 ± 0.0014	HQ: FFS $N_f = 3$
A.Hoang et al.	$0.1135 \pm 0.0011 \pm 0.0006$	e^+e^- thrust
ABKM	0.1129 ± 0.0014	HQ: BSMN-approach
BBG (2006)	$0.1134\ ^{+0.0019}_{-0.0021}$	valence analysis, NNLO
JR (2008)	0.1124 ± 0.0020	dynamical approach
MSTW (2008)	0.1171 ± 0.0014	
H1/ZEUS (2010)	0.1145 ± 0.0042	(combined H1/ZEUS data, prelimiary)
ABM (2010)	0.1147 ± 0.0012	(FFN, combined H1/ZEUS data in)
BBG (2006)	$0.1141\ ^{+0.0020}_{-0.0022}$	valence analysis, N^{3}LO
WA (2009)	0.1184 ± 0.0007	

$\alpha_s(M_Z^2)$ and $\Lambda^{(4)}_{\rm QCD}$

$$\Lambda^{(4)}_{\rm QCD} = 243.5 \pm 62\ (\exp)\ {}^{-37}_{+21}\ ({\rm FS})\ {}^{+46}_{-87}\ ({\rm RS}).$$

$$\alpha_s(M_Z^2) = 0.1132\ {}^{+0.0043}_{-0.0051}\ (\exp)\ {}^{-0.0029}_{+0.0015}\ ({\rm FS})\ {}^{+0.0032}_{-0.0075}\ ({\rm RS})\ .$$

Earlier values :

$$\text{E154}: \quad \alpha_s(M_Z^2) = 0.108 - 0.116$$

$$\text{SMC}: \quad \alpha_s(M_Z^2) = 0.121 \pm 0.007$$

$$\text{ABFR}: \quad \alpha_s(M_Z^2) = 0.120\ {}^{+0.100}_{-0.008}$$

$$\text{BB02}: \quad \alpha_s(M_Z^2) = 0.114\ {}^{+0.100}_{-0.008}$$

$\alpha_s(M_Z^2)$

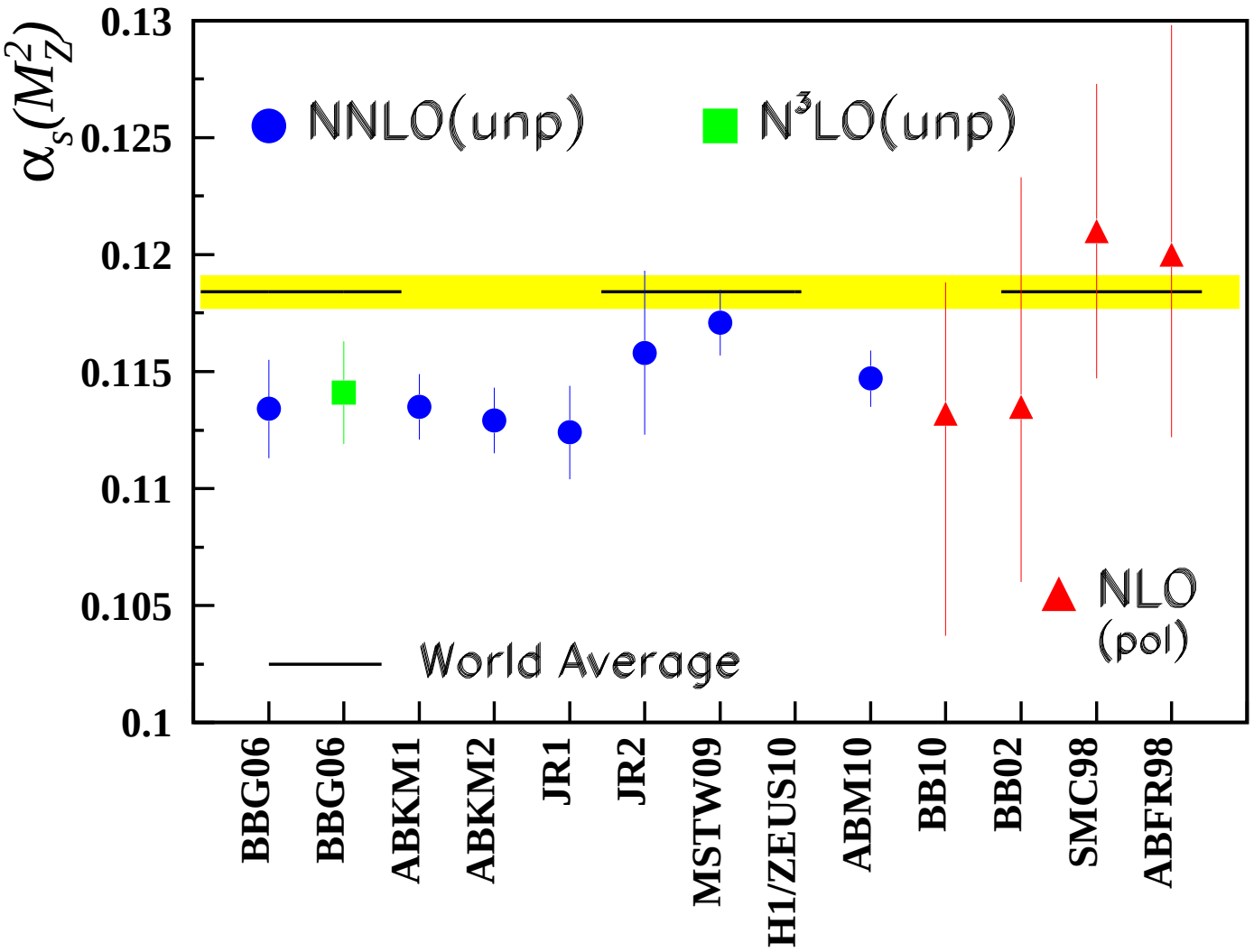

World average: S. Bethke, Eur.Phys.J.C64:689-703,2009; yellow band.

Higher Twist

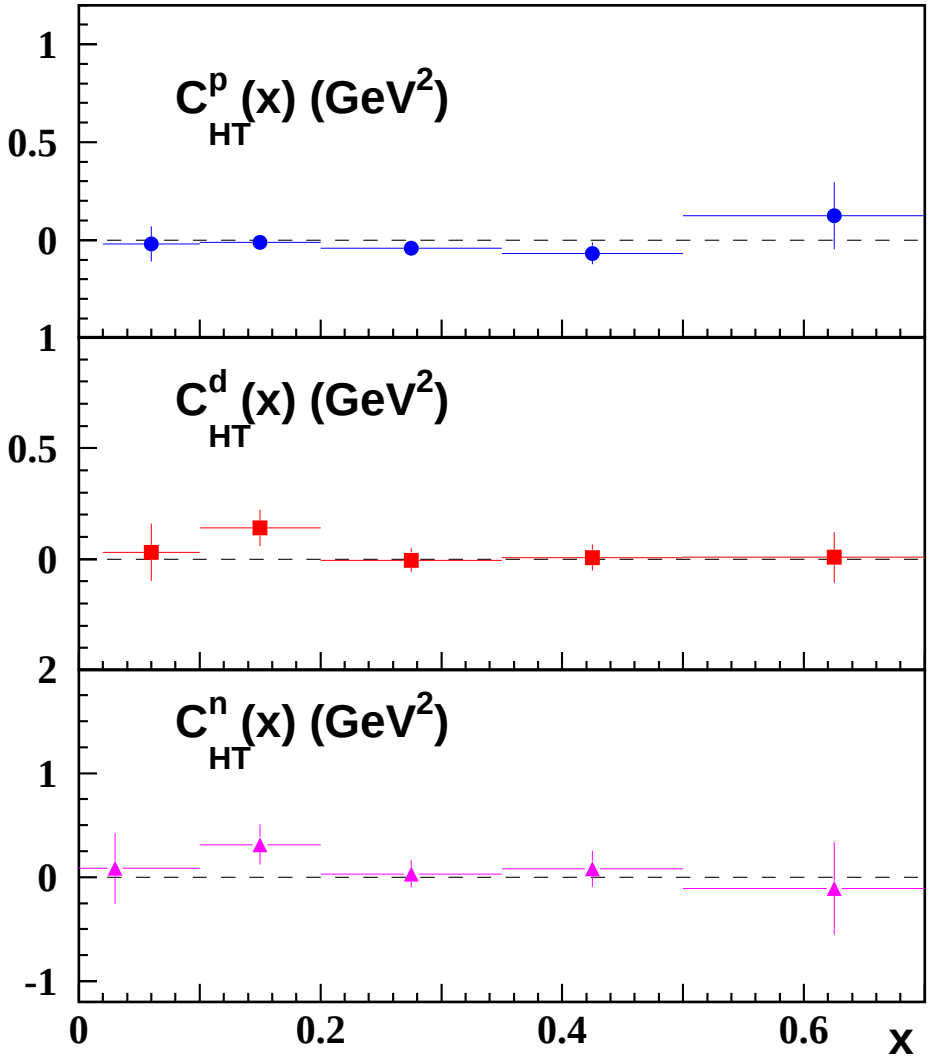

Figure 7: The higher twist coefficients $C_i^p(x)$, $C_i^d(x)$ and $C_i^n(x)$ as function of x.

$$g_1(x,Q^2) = g_1^{\rm LT}(x,Q^2)\left[1+\frac{C_{\rm HT}(x)}{Q^2}\right]$$

Higher Twist

$< x >$	$C_i^p, [\mathrm{GeV}^2]$	$C_i^d, [\mathrm{GeV}^2]$
0.060	-0.020 $\pm$ 0.089	0.030 $\pm$ 0.131
0.150	-0.010 $\pm$ 0.036	0.140 $\pm$ 0.082
0.275	-0.041 $\pm$ 0.027	-0.005 $\pm$ 0.054
0.425	-0.068 $\pm$ 0.055	0.007 $\pm$ 0.059
0.625	0.124 $\pm$ 0.172	0.008 $\pm$ 0.114

Table 5: The higher twist coefficients $C_i^p(x)$ and $C_i^d(x)$ as function of x.

Conclusions

- An NLO analysis of the current polarized DIS World data has been performed accounting for all parameter correlations.
- Grids including correlated errors of the parameterization are provided.
- The gluon density comes out lower than in previous analyses.
- $\Lambda^{(4)}_{\rm QCD}$ and $\alpha_s(M_Z^2)$ have been measured. Similar central values as in the BB02 analysis and recent N$^{2(3)}$LO DIS unpolarized world data analyses are obtained. The NLO FS/RS variations still imply a large uncertainty at NLO if compared to the experimental error.
- We determined the higher twist contributions which are found to be compatible with zero within the present errors both for proton and deuteron targets.
- NLO Moments with correlated errors can be provided for comparisons with LGT simulations.